

Research Paper/

Machine-Learning Methods for Water Table Depth Prediction in Seasonal Freezing-Thawing Areas

Tianxing Zhao¹, Yan Zhu^{1,*}, Ming Ye², Wei Mao¹, Xiaoping Zhang³, Jinzhong Yang¹, Jingwei Wu¹

¹State Key Laboratory of Water Resources and Hydropower Engineering Science, Wuhan University, Wuhan, Hubei 430072, China

²Department of Earth, Ocean, and Atmospheric Science, Florida State University, Tallahassee, FL 32306, USA

³School of Mathematics and Statistics, Wuhan University, Wuhan, Hubei, 430072, P.R. China

Corresponding Author. Phone: 86-2768775432; Email: zyan0701@163.com; Fax: 86-2768776001

Conflict of interest: None.

Article Impact Statement: Water table depth prediction in seasonal freezing-thawing area, using integrated machine-learning methods with and without temperature data.

May 2019

For publication in Groundwater

This article has been accepted for publication and undergone full peer review but has not been through the copyediting, typesetting, pagination and proofreading process, which may lead to differences between this version and the Version of Record. Please cite this article as doi: 10.1111/gwat.12913

Accepted Article

Abstract: Long-term and accurate predictions of regional groundwater hydrology are important for maintaining environmental sustainability in arid agricultural areas that experience seasonal freezing and thawing where serious water-saving measurements are used. In this study, we firstly developed a machine-learning method by integrating a multivariate time series controlled auto-regressive method and the ridge regression method (CAR-RR) for water table depth modeling. We applied and evaluated this model in the Hetao Irrigation District, located in northwest China where the freezing-thawing period is five months long. To train and validate the model, we used monthly data of water diversion, precipitation, evaporation and drainage from 1995 to 2013. The CAR-RR model yielded more accurate results than the support vector regression (SVR) and multiple linear regression (MLR) models did in the validation period. To extend the model applicability during freezing-thawing periods, we included additional temperature information. We compared results obtained using temperature only during the freezing-thawing period with results obtained without temperature, which showed that the input data of the temperature during the freezing-thawing period significantly improved the model accuracy. To resolve the problem of capturing the peaks and troughs of CAR-RR, we further developed an integrated CAR-SVR model to consider the nonlinearity. The optimal model (CAR-SVR) was then used to predict the water table depth under future water-saving measurements. It demonstrated that water diversion was the most important factor affecting the water table depth. A water table depth with less than 3.64 billion m³ water diversion will result in risks of environment problems.

Key words: machine-learning method; integrated CAR-RR; CAR-SVR; seasonal freezing-thawing area; water table depth.

Introduction

When using groundwater resource to support various human activities (Yoon et al., 2016), groundwater overexploitation has occurred in many regions of the world and has caused serious water-level decline (Rodell et al., 2009; Ebrahimi and Rajaei, 2017). Effective and efficient groundwater management has become more and more important because of the ever-increasing water demand to meet industrial, agricultural, and domestic needs (Suryanarayana et al., 2014). Efficient management requires accurate and reliable prediction of groundwater dynamics, and one important variable for characterizing groundwater dynamics is evolution of water table depth. Water table depth predictions can be obtained using either physically based modeling approaches or statistically based machine-learning approaches. In the past several decades, numerous physically based groundwater models have been utilized to predict groundwater dynamics, including those developed by using software such as MODFLOW (Coppola et al., 2003), FEFLOW (Feng et al., 2011), HYDROGEOSPHERE (Brunner et al., 2012), Hydrus (Satchithanantham et al., 2014), and Q3D (Zhu et al., 2012). Field applications of these models, however, are difficult because of the lack of data to characterize the spatial heterogeneity of groundwater aquifers and temporal changes of boundary conditions, especially at the regional scale; the computational cost of executing these physically based models is also a significant concern (Raghavendra and Deka, 2014).

Machine-learning methods provide an alternative way to make groundwater predictions when inadequate information is available or when forecasting efficiency is desired (Daliakopoulos et al., 2005; Coppola et al., 2005; Shiri et al., 2013). Machine-learning models can reveal hidden patterns

(e.g., nonlinearity and nonstationarity) of complicated hydrological systems based on available data, and use these patterns to make predictions (Sahoo et al., 2017; Rezaie-Balf et al., 2017). A variety of models based on machine-learning methods have been developed for hydrological predictions, including artificial neural network (ANN; Daliakopoulos et al., 2005; Kuo et al., 2007), autoregressive models (Yang et al., 2009; Shirmohammadi et al., 2013), support vector machine (SVM; Behzad et al., 2009; Yoon et al., 2011), and genetic algorithms (GA; Jha and Sahoo, 2015; Ravansalar et al., 2017). Daliakopoulos et al. (2005), for example, developed an optimal ANN architecture to simulate the decreasing trends of groundwater levels. Kuo et al. (2007) used ANN to predict reservoir eutrophication. Yang et al. (2009) used the integrated time series (ITS) and back-propagation ANN (BPANN) methods to forecast groundwater levels. Yoon et al. (2011) used ANN and SVM to predict groundwater levels in a coastal aquifer. These previous works demonstrate the capacity and applicability of machine-learning methods to capture the nonlinear relation between the inputs and outputs of hydrologic systems. Machine-learning methods may achieve comparable or even more accurate results than physically based models, with less computational cost and data demand (Coulibaly et al., 2001; Coppola et al., 2003; Mohanty et al., 2013).

This study is focused on the use of machine-learning methods to predict water table depth in agricultural areas where water table exhibits seasonality and temporal fluctuations resulting from the impacts of climate, land uses, and irrigations (Knapp et al., 2003; Schoups et al., 2005; Shah et al., 2009). Because water table depth is related to previous hydrologic conditions with possibly a large time lag, water table dynamics cannot be predicted easily by many machine-learning methods directly (Chen et al., 2002; Nayak et al., 2006). To handle historical data, the data should be

Accepted Article

pre-processed before being used by machine-learning models. Therefore, it is necessary to integrate a pre-processing method (e.g., wavelet method) with the machine-learning methods (e.g., SVM and ANN) to develop hybrid machine-learning methods (Maheswaran and Khosa, 2013; Moosavi et al., 2014; Ebrahimi and Rajaei, 2017). In these hybrid methods, wavelet analysis and singular spectrum analysis are used to decompose nonstationary and nonlinear time series data into a set of simpler and easier-to-model data, which makes the hybrid models adaptive and intuitive for handling time lags in time-dependent data (Huang et al., 2014; Zhang et al., 2015; Sahoo et al., 2017). After decomposing the data, the machine-learning methods can further be used for simulating and forecasting, which is complicated.

Using multivariate time series is useful for simulating fluctuations in the dependent variables of a hydrologic system, as groundwater dynamics are determined by multiple variables (Nourani et al., 2008; Manzione et al., 2012; Russo and Lall, 2017). The controlled auto-regressive (CAR) method is usually adopted to handle multivariate time series, and it can well describe time-dependent variables and evaluate the importance of new observational data (Chang et al., 2008). Yao et al. (2014) proposed a runoff CAR model to explore responses of runoff to climate change and human activities for water resource management. Zhang et al. (2017) developed a CAR model for groundwater-level prediction. The model failed for future prediction because of an overfitting problem, which was caused by the multicollinearity of variables when a higher-order model with too many variables was used.

In this study, we developed hybrid machine-learning models to simulate and predict the water table depth in agricultural areas with a seasonal freezing and thawing period. We used the CAR

Accepted Article

model to handle multivariate time series for groundwater prediction. We firstly integrated the ridge regression (RR) method with CAR to solve the problem of unstable and/or biased coefficient estimates caused by multicollinearity in regression analysis when significant correlations exist among input variables. Another concern to develop the CAR-RR model was the capability of the model to show the intrinsic relationship of the dependent variable with the independent variables, which is convenient for application. The integrated CAR-RR model is trained and validated by the monthly data obtained during the period from 1995 to 2013 in the Hetao Irrigation District. We compared the results obtained from the CAR-RR model with those obtained using other machine-learning models without data preprocessing, specifically speaking, support vector regression (SVR) and multiple linear regression (MLR). Moreover, to improve the simulation accuracy for freezing-thawing period, we considered temperature as an additional variable. We then compared the simulated results that considered temperature only during the freezing-thawing period and evaluated these results with those without temperature. In order to better capture the peaks and troughs, we further integrated CAR with SVR, because the latter considers the nonlinearity between water table depth and the input variables used by CAR. Since CAR-SVR outperforms CAR-RR, the former was used to predict water table depth under nine scenarios with three different irrigation water diversions and future precipitation.

Study area and observation data

Study area

The Hetao Irrigation District is located in the west of the Inner Mongolia Autonomous Region (Figure 1). The district is located in an arid climate area, with an average annual precipitation of 152

mm and an average annual evaporation of 2,400 mm (measured by using 20 cm-diameter evaporation pans). The irrigation water in this district is mainly from the water diversion from Yellow River and precipitation. As shown in Figure 1, 227 groundwater observation wells are distributed across the district, and the water table depth is measured every 5 days. Because of serious water resource scarcity in northern China, a water-saving plan for the Hetao Irrigation District was proposed in 1999, and the amount of water allocated to the irrigation district will be reduced from 4.60 billion m³ first to 4 billion m³ and finally to 3.64 billion m³. Furthermore, this district has more than five months in its freezing-thawing period. The mechanisms governing the movement of groundwater and soil water during the freezing-thawing period are substantially different from those in the non-freezing-thawing period (Wei et al., 2016), which is controlled by temperature and difficult to evaluate according to physically based models. Therefore, it is a significant challenge to investigate the water table depth change under different water-saving measurements in this seasonal freezing-thawing agricultural district.

Data description

The original data included the water diversion for irrigation, precipitation, evaporation, temperature, water drainage, and water table depth from 1995 to 2013, as shown in Figure 2. We used Student's *t*-test to determine the important variables considering the significance of the independent variables, while also eliminating the insignificant variables (Sahoo and Jha, 2013). The precipitation and evaporation data are the monthly sum of the entire irrigation district and were obtained from the *Water Conservancy Data Compilation in the Hetao Irrigation District* (1995–2013). We used the evaporation other than evapotranspiration because there are no measurements for

evapotranspiration in this area. The water diversion and water drainage data are the monthly amount based on the water conservancy statistics for Bayannur City, which are measurements derived from the diversion sluice and surface drains as shown in Figure 1. The monthly average temperature data are from the statistics of meteorological data in the Hetao Irrigation District (1995–2000) and the China Meteorological Data Service Center (2000–2013). The water table depth data are the monthly average value of all wells. Because these data vary widely in scales (units), as shown in Figure 2, we standardized the original data in the calibration period to eliminate any errors caused by inconsistent scales (units) of the features, as shown in Figure 2.

Data pre-processing

The correlation coefficients of the five independent variables (water diversion, x_1 ; precipitation, x_2 ; evaporation, x_3 ; water drainage, x_4 ; temperature, x_5) are quantified as shown in Table 1. The table shows that the water drainage and evaporation are highly related to water diversion, and that the evaporation is closely related to temperature.

Table 1 Correlation coefficients between independent variables.

	x_1	x_2	x_3	x_4	x_5
x_1	1.0000				
x_2	0.2361	1.0000			
x_3	0.5063	0.4409	1.0000		
x_4	0.5631	0.1061	0.2017	1.0000	
x_5	0.5888	0.6020	0.9252	0.2985	1.0000

The condition index is used to quantify the multicollinearity among input variables, which is calculated as follows (Demirhan, 2014):

$$\kappa = \sqrt{\lambda_1 / \lambda_q} , \quad (1)$$

where $\lambda_1 \geq \lambda_2 \geq \dots \geq \lambda_5$ are the eigenvalues of $(\mathbf{X}^*)^T \mathbf{X}^*$; \mathbf{X}^* is a $n \times 5$ matrix of the standardized input variables x_1, x_2, x_3, x_4 , and x_5 . The calculated largest κ value is 42.57, indicating strong multicollinearity among these input variables.

Methodologies

Machine-learning models

CAR model for multivariate time series

An m -order autoregressive time series model with q independent variables and one dependent variable can be described by the following equations:

$$y_s = \boldsymbol{\beta} \boldsymbol{\theta}_s + \varepsilon_s, \quad (2)$$

$$\boldsymbol{\theta}_s = (\boldsymbol{\Gamma}^T, \mathbf{X}_1^T, \mathbf{X}_2^T, \dots, \mathbf{X}_q^T)^T, \quad (3a)$$

$$\boldsymbol{\Gamma} = (1, y_{s-1}, y_{s-2}, \dots, y_{s-m})^T, \quad (3b)$$

$$\mathbf{X}_i = (x_{i,s}, x_{i,s-1}, x_{i,s-2}, \dots, x_{i,s-m})^T, (i=1, 2, \dots, q), \quad (3c)$$

$$\boldsymbol{\beta} = (\gamma, \boldsymbol{\chi}_1, \boldsymbol{\chi}_2, \dots, \boldsymbol{\chi}_q), \quad (4a)$$

$$\boldsymbol{\gamma} = (\beta_0, \beta_1, \beta_2, \dots, \beta_m), \quad (4b)$$

$$\boldsymbol{\chi}_i = (\beta_{i,0}, \beta_{i,1}, \beta_{i,2}, \dots, \beta_{i,m}), (i=1, 2, \dots, q), \quad (4c)$$

where y_s is the dependent variable of the s -th month (the current time); m is the lag number; y_{s-m} is the dependent variable with the lag of m months; q is the number of independent variable; $x_{i,s-m}$ is the i -th independent variable with the lag of m months; y_{s-m} and $x_{i,s-m}$ are a pair of time series data; β_m and $\beta_{i,m}$ are unknown parameters; ε_s is the random variable; $\boldsymbol{\theta}_s$ is a vector of known numbers and variables; $\boldsymbol{\beta}$ is the vector of unknown parameters; $\boldsymbol{\Gamma}$ is the vector consisting of constant 1 and variables of the dependent variable of different lags; and \mathbf{X}_i is the vector of the i -th independent variable with different lags. For Eq. (4), the unknowns are the vector $\boldsymbol{\beta}$, consisting of $\boldsymbol{\gamma}$ (the parameters of $\boldsymbol{\Gamma}$) and $\boldsymbol{\chi}_i$ (the parameters of \mathbf{X}_i).

RR model

The unknown parameters, β , of the previously given linear model can be estimated using the least square techniques. The equations for the estimate are as follows:

$$\beta = (\mathbf{W}^T \mathbf{W})^{-1} \mathbf{W}^T \mathbf{Y}, \quad (5a)$$

$$\mathbf{W} = (\theta_n, \theta_{n-1}, \theta_{n-2}, \dots, \theta_{m+1})^T, \quad (5b)$$

$$\mathbf{Y} = (y_n, y_{n-1}, y_{n-2}, \dots, y_{m+1})^T, \quad (5c)$$

where $\hat{\beta}$ is the vector of estimated values of the unknown parameters; \mathbf{W} is the matrix of θ ; \mathbf{Y} is the vector of dependent variables in Eq. (2); and n is the number of observations (i.e., the number of times).

The parameter estimates obtained by using Eq. (5a) are unbiased, that is, the expectation of $\hat{\beta}$ ($E(\hat{\beta})$) equals β . The term $\mathbf{W}^T \mathbf{W}$ is close to 0 when the correlation between the independent variables is strong, which will cause a large error when calculating the inverse of $\mathbf{W}^T \mathbf{W}$. The essence of the RR model is to artificially add a non-negative factor to the main diagonal element of the matrix $\mathbf{W}^T \mathbf{W}$.

The modified Eq. (5a) is

$$\beta = (\mathbf{W}^T \mathbf{W} + k\mathbf{I})^{-1} \mathbf{W}^T \mathbf{Y}, \quad (6)$$

where k is a ridge constant; \mathbf{I} is the identity matrix. The obtained parameters by using Eq. (6) are biased. The RR model can avoid overfitting problem by adding the non-negative factor, which introduces a priori distribution on the model parameters.

MLR model

The MLR model is as follows (Makridakis et al., 2008; Sahoo and Jha, 2013):

$$y_s = \eta \mathbf{H} + \varepsilon_s, \quad (7a)$$

$$\mathbf{H} = (1, x_1, x_2, \dots, x_q)^T, \quad (7b)$$

$$\boldsymbol{\eta} = (\beta_0, \beta_1, \beta_2, \dots, \beta_q), \quad (7c)$$

where y_s is the dependent variable; $x_j (j=1, 2, \dots, q)$ represents the j -th independent variable; q is the number of the independent variables; $\beta_j (j=0, 1, 2, \dots, q)$ is the j -th unknown parameter; and ε_s is the random variable that is normally distributed. For MLR, $\boldsymbol{\eta}$ is unknown, and \mathbf{H} is known. The unknown parameters, $\boldsymbol{\eta} = (\beta_0, \beta_1, \beta_2, \dots, \beta_q)$, can be estimated by applying the least-square technique to minimize the sum of squares of the difference between the actual observations and the corresponding model simulations (Makridakis et al., 2008).

SVR model

Building an SVR model requires selecting the support vectors and determining their weights (Khan and Coulibaly, 2006; Behzad et al., 2010). The process of an SVR estimator (f) on regression can be expressed as follows (Shiri et al., 2013):

$$f(\mathbf{v}) = \mathbf{u}\varphi(\mathbf{v}) + b, \quad (8)$$

where \mathbf{u} is a weight vector; \mathbf{v} is the input vector; φ is a nonlinear transfer function mapping the input space into a high-dimensional feature space; and b is a bias correction term. Eq. (8) is solved by introducing an object function of convex optimization with ζ -insensitivity loss function (Vapnik, 1995), as follows:

$$\begin{aligned} \min_{\mathbf{u}, b, \zeta, \zeta^*} \quad & \frac{1}{2} \|\mathbf{u}\|^2 + C \sum_{i=1}^N (\zeta_i + \zeta_i^*), \quad (C > 0) \\ \text{subject to} \quad & \begin{cases} y_i - \mathbf{u}\varphi(\mathbf{v}_i) - b \leq \zeta + \zeta_i \\ \mathbf{u}\varphi(\mathbf{v}_i) + b - y_i \leq \zeta + \zeta_i^*, \quad (i = 1, 2, \dots, N) \\ \zeta_i, \zeta_i^* \geq 0 \end{cases}, \end{aligned} \quad (9)$$

where ζ_i and ζ_i^* are slack variables penalizing the estimation error by the ζ -insensitivity loss function; N is the number of support vectors; and C is a positive constant influencing the degree of penalizing loss when a training error occurs. By minimizing the regularization term $\mathbf{u}^2/2$, we avoided

underfitting and overfitting to train the data. We dealt with the optimization problem by constructing a Lagrangian function from the primal objective function and by inducing the kernel function, as follows:

$$\begin{aligned} \min_{\sigma_i, \sigma_i^*} \quad & \frac{1}{2} \sum_{i,j=1}^N (\sigma_i - \sigma_i^*)(\sigma_j - \sigma_j^*) K(\mathbf{v}_i, \mathbf{v}_j) + \zeta \sum_{i=1}^N (\sigma_i + \sigma_i^*) - \sum_{i=1}^N y_i (\sigma_i - \sigma_i^*) \\ \text{subject to} \quad & \begin{cases} \sum_{i=1}^N (\sigma_i - \sigma_i^*) = 0 \\ 0 \leq \sigma_i, \sigma_i^* \leq C \end{cases}, \\ \text{to obtain} \quad & f(\mathbf{v}) = \sum_{i=1}^N (\sigma_i - \sigma_i^*) K(\mathbf{v}_i, \mathbf{v}_j) + b \end{aligned} \quad (10)$$

where σ_i and σ_i^* are Lagrangian multipliers; $K(\mathbf{v}_i, \mathbf{v}_j)$ is the kernel function which can be a linear function, polynomial function, radial basis function, or sigmoid function.

Integrated CAR-RR and CAR-SVR models

Figure 3 is the flow chart of the integrated CAR-RR and CAR-SVR models. First, all standardized independent variables are imported to the CAR model. When developing the CAR-RR model, the vector of unknown parameters β is then obtained by the RR model as shown in Eq. (6). While developing the CAR-SVR model, the vector θ_s determined by the CAR model are imported to the SVR model as the input vector \mathbf{v} . And then the Eq. (8) are solved by Eq. (9) and Eq. (10). The order of the CAR-RR (CAR-SVR) model is determined by the F test. The F test of the m and $m+1$ order CAR-RR (CAR-SVR) model is defined as follows (Tang, 2010):

$$F = \frac{RSS_m - RSS_{m+1}}{RSS_{m+1}} \times \frac{d_{m+1}}{d_m - d_{m+1}} \sim F_\alpha(d_m - d_{m+1}, d_{m+1}), \quad (11)$$

where RSS is the residual sum of squares of the CAR-RR (CAR-SVR) model; d is the model's freedom degree; and α is the confidence level, generally $\alpha = 0.05$. If $F < F_\alpha(d_m - d_{m+1}, d_{m+1})$, it means that the m -order model is the appropriated one. Otherwise, the model with $m+1$ order needs to be

developed. After determining the model order, we carried out Student's t -test to consider the significance of the independent variables of the CAR-RR model, and then to eliminate the insignificant independent variables. We again solved the model without insignificant independent variables to obtain the new parameter estimates of the CAR-RR model, as shown in Figure 3(a).

Model evaluation and test

Model evaluation metrics

To evaluate the simulation accuracy of the previous models and the deviation between simulated and observed values, three statistical metrics, including coefficient of multiple determination R^2 , root mean square error ($RMSE$), and Akaike information criterion (AIC), are defined as follows:

$$R^2 = \frac{\sum_{i=1}^{nu} (y_i - \bar{y})^2}{\sum_{i=1}^{nu} (y_i - \hat{y}_i)^2}, \quad (12)$$

$$RMSE = \sqrt{\frac{\sum_{i=1}^{nu} (y_i - \hat{y}_i)^2}{nu}}, \quad (13)$$

$$AIC = -2 \times I + 2 \times NP, \quad (14a)$$

$$I = -\frac{nu}{2} \times [\ln(2 \times \pi) + \ln(\frac{RSS}{nu}) + 1], \quad (14b)$$

where y_i is the observed value of the dependent variable; \bar{y} is the mean of the observed values of the dependent variable; \hat{y}_i is the estimated or predicted value of y_i ; nu is the number of measurements in the evaluation period; I is the log likelihood; NP is the number of parameters estimated; and RSS is the residual sum of squares. The R^2 value close to 1.0, and the $RMSE$ value close to 0 show the accuracy of the model. The relative smaller AIC value indicates the modeling results are more accurate.

Residual normality test

Because the previous linear regression equations assume that the residual term follows the normal distribution, a normality test on the residuals is necessary. We conducted the normality test using the Lilliefors test, in which we used the sample mean and variance without knowing the population mean and variance of the residuals. This Lilliefors test requires the evaluation of two test statistics, D and the p -value (Lilliefors, 1967; Wang et al., 2016). When D was closer to 0 and the p -value as larger than the significance level α (usually with the value of 0.05), the residual of the sample data was closer to normal distribution, which qualified the model assumption.

Model application

We used data from the Hetao Irrigation District for the period from 1995 to 2005 for model calibration, and used data for the period from 2006 to 2013 for model validation. Given the policy of reducing the water diversion from the Yellow River, we considered three scenarios of water diversion in the prediction, marked as W1 (with the current water diversion of 4.60 billion m^3), W2 (4.00 billion m^3), and W3 (3.64 billion m^3). Because water drainage is highly related to water diversion as shown in Table 1, we set the water drainages as 0.3 billion m^3 , 0.15 billion m^3 , 0.05 billion m^3 under the W1, W2 and W3 scenarios. We considered three different levels of precipitation assurance representing rainy, medium and drought hydrological years (25%, P1; 50%, P2; 75%, P3). Because the evaporation in the Hetao Irrigation District is relatively stable annually as shown in Figure 2, we used the average evaporation from the data set from 1995 to 2013. Therefore, the nine prediction scenarios composed of different water diversion and precipitation assurance levels are marked as S1 (P1W1), S2 (P2W1), S3 (P3W1), S4 (P1W2), S5 (P2W2), S6 (P3W2), S7 (P1W3), S8 (P2W3), and

S9 (P3W3).

Results and discussion

We established the CAR-RR model to simulate the variation of the water table depth, and compared the results with those from MLR, SVR, and the traditional CAR models. We imported the temperature during the freezing-thawing period into the CAR-RR model to improve the simulation results, marked as CAR-RR(FT). We discussed limitations of the CAR-RR(FT) model and improved the model to consider the nonlinearity of variables by integrating the CAR with SVR, and used the optimal CAR-SVR(FT) model to predict variations in the water table depth according to the future water-saving policy.

Results of the CAR-RR model

The model order was $m = 2$, according to F test when we developed the CAR-RR model. We then selected the model parameters according to Student's t -test. Because the temperature variable (x_5) cannot pass the Student's t -test, the CAR-RR model has only four input variables. The variables and parameters are listed in Table 2. Note that the observed water table depth data from lag time are used in the calibration period to obtain the parameters, whereas the predicted data are used in the validation and prediction periods. We compared the calculated water table depths of the CAR-RR model in the calibration and validation periods with the observations, as shown in Figure 4. The evaluation statistics, R^2 , $RMSE$ and AIC were 0.9489, 0.0886 m, and -238.3, respectively, in the calibration period, and 0.8230, 0.1896 m, and -23.8, respectively, in the validation period, which demonstrated the satisfactory performance of the developed model. The results of the Lilliefors test were $D = 0.0462$, $p\text{-value} = 0.7107$, which showed the effectiveness of the integrated CAR-RR

model.

Table 2 The simulated equations.

Simulated method	Simulated form	Variables	Values of parameters
CAR-RR	$y_s = \boldsymbol{\beta}\boldsymbol{\theta}_s = \mathbf{r}\boldsymbol{\Gamma} + \sum_{i=1}^4 \boldsymbol{\chi}_i \mathbf{X}_i$	$\boldsymbol{\Gamma} = (1, y_{s-1}, y_{s-2})^T$ $\mathbf{X}_i = (x_{i,s}, x_{i,s-1}, x_{i,s-2})^T$	$\mathbf{r} = (1.641, 5.484 \times 10^{-1}, -3.180 \times 10^{-1})$; $\boldsymbol{\chi}_1 = (-2.041 \times 10^{-3}, -1.490 \times 10^{-3}, 0)$; $\boldsymbol{\chi}_2 = (-2.123 \times 10^{-3}, -1.875 \times 10^{-3}, 0)$; $\boldsymbol{\chi}_3 = (-3.874 \times 10^{-4}, 0, 2.066 \times 10^{-3})$; $\boldsymbol{\chi}_4 = (-4.420 \times 10^{-2}, -7.145 \times 10^{-3}, -1.629 \times 10^{-2})$
MLR	$y_s = \boldsymbol{\eta}\mathbf{H}$	$\mathbf{H} = (1, x_1, x_2, x_3, x_4)^T$	$\boldsymbol{\eta} = (2.081, 1.675 \times 10^{-3}, -3.013 \times 10^{-4}, 0, -8.282 \times 10^{-1})$
CAR	$y_s = \mathbf{r}\boldsymbol{\Gamma} + \sum_{i=1}^4 \boldsymbol{\chi}_i \mathbf{X}_i$	$\boldsymbol{\Gamma} = (1, y_{s-1}, y_{s-2}, y_{s-3}, y_{s-4})^T$ $\mathbf{X}_i = (x_{i,s}, x_{i,s-1}, x_{i,s-2}, x_{i,s-3}, x_{i,s-4})^T$	$\boldsymbol{\gamma} = (-1.051 \times 10^{-1}, 1.232, -7.123 \times 10^{-1}, 2.708 \times 10^{-1}, 2.106 \times 10^{-1})$; $\boldsymbol{\chi}_1 = (-2.778 \times 10^{-3}, -1.122 \times 10^{-3}, 9.233 \times 10^{-4}, 9.679 \times 10^{-4}, 1.015 \times 10^{-3})$; $\boldsymbol{\chi}_2 = (-2.448 \times 10^{-3}, 0, 5.846 \times 10^{-4}, 3.584 \times 10^{-4}, 9.503 \times 10^{-4})$; $\boldsymbol{\chi}_3 = (0, 8.857 \times 10^{-4}, 1.938 \times 10^{-3}, -1.529 \times 10^{-3}, 0)$; $\boldsymbol{\chi}_4 = (-3.546 \times 10^{-2}, 2.326 \times 10^{-2}, -1.160 \times 10^{-2}, 0, 2.724 \times 10^{-2})$
CAR-RR(FT)	$y_s = \mathbf{r}\boldsymbol{\Gamma} + \sum_{i=1}^5 \boldsymbol{\chi}_i \mathbf{X}_i$	$\boldsymbol{\Gamma} = (1, y_{s-1}, y_{s-2}, y_{s-3})^T$ $\mathbf{X}_i = (x_{i,s}, x_{i,s-1}, x_{i,s-2}, x_{i,s-3})^T$	$\boldsymbol{\gamma} = (1.064, 5.463 \times 10^{-1}, 0, -9.149 \times 10^{-2})$; $\boldsymbol{\chi}_1 = (-1.719 \times 10^{-3}, -2.690 \times 10^{-3}, 0, 0)$; $\boldsymbol{\chi}_2 = (0, -2.030 \times 10^{-3}, 0, 0)$; $\boldsymbol{\chi}_3 = (0, 0, 1.865 \times 10^{-3}, 0)$; $\boldsymbol{\chi}_4 = (-3.429 \times 10^{-2}, 0, 0, 0)$; $\boldsymbol{\chi}_5 = (0, -1.814 \times 10^{-2}, 0, 0)$

Model comparison results

We developed the machine-learning models based on MLR, SVR and traditional CAR for water table depth prediction with input variables of water diversion, precipitation, evaporation, and water drainage. To ensure consistency of the input data with data used by CAR-RR model, we did not include temperature data. The MLR and CAR models are listed in Table 2. We used the ε -SVR model in the study. We selected the best kernel function and parameters by using a tuning function. We obtained the SVR model using the svm function. The kernel function was RBF, and the penalty coefficient C was 10, gamma was 0.5, and the accuracy of the iterative computation ε was 0.01.

The comparison results between the measured and simulated water table depth in the calibration and validation periods by various machine-learning methods are displayed in Figure 4. We compared the performance of CAR-RR, CAR, MLR, and SVR using relative error distribution and the evaluation indicators. SVR was the best model in the calibration period with 94% of the relative errors less than 10%, and the corresponding value was 92% for CAR-RR, 91% for CAR, and 57% for MLR. The CAR-RR model was the best model in the validation period, however, with 73% of the relative errors less than 10%, and the corresponding value was 57% for SVR, 56% for CAR, and 51% for MLR. The MLR model performed the worst in the calibration and validation periods. The evaluation statistics (R^2 , $RMSE$, and AIC) of the four models showed that the CAR model ($R^2 = 0.9559$, $RMSE = 0.0815$ m, $AIC = -237.7$) and the SVR model ($R^2 = 0.9494$, $RMSE = 0.0872$ m, $AIC = -260.6$) were slightly better than the CAR-RR model ($R^2 = 0.9489$, $RMSE = 0.0886$ m, $AIC = -238.3$) in the calibration period, and the MLR model ($R^2 = 0.7185$, $RMSE = 0.2049$ m, $AIC = -37.0$) had the worst performance. The CAR-RR model ($R^2 = 0.8230$, $RMSE = 0.1896$ m, $AIC = -23.8$)

yielded better results in the validation period, followed first by the SVR model ($R^2 = 0.7067$, $RMSE = 0.2074$ m, $AIC = -20.6$), then by the CAR model ($R^2 = 0.8482$, $RMSE = 0.2182$ m, $AIC = 21.1$) and last by the MLR model ($R^2 = 0.6149$, $RMSE = 0.2553$ m, $AIC = 17.3$). In summary, the CAR-RR model was considered to be a reasonable model for predicting water table depth.

Improvement of the CAR-RR model during the freezing-thawing period

The Hetao Irrigation District, experiences little precipitation and no water diversion during the freezing-thawing period (Yang et al., 2017). During the freezing period, the upper-layer soil water is frozen at negative temperatures, which leads to a sharp decrease in the matric potential in the soil zone, causing the groundwater migration to the upper frozen soil. When the temperature rises, the frozen ice in the soil melts from both the upper and lower directions to the middle, and the melting water recharges the groundwater (Li et al., 2012). Therefore, temperature is the major concern to control the water table depth during the freezing-thawing period. We did not consider it as an input variable when developing the CAR-RR model in the section titled Results of the CAR-RR model because it cannot pass Student's t -test. Considering the physical mechanism, we used the temperature only during the freezing-thawing period as an input variable, and set it as 0 during the remainder of the time. We developed the new CAR-RR model (marked as CAR-RR(FT)) according to the model development procedure in the section titled Machine-learning models with the pre-processed temperature data. In this case, all five variables passed Student's t -test. The order of CAR-RR(FT) model was $m = 3$, as suggested by the F test. We selected the model parameters according to Student's t -test as shown in Table 2.

The simulation results of the CAR-RR model and CAR-RR(FT) model are shown in Figure 4.

Figure 4(a) shows that the CAR-RR(FT) model had a better performance during the freezing-thawing period and captured the peaks of the water table depth satisfactorily. The evaluation statistics (R^2 , $RMSE$, and AIC) of the two models during the freezing-thawing period and throughout the whole simulation period are given in Figures 4(b), 4(c), 4(g), 4(h), and 4(l)-4(o). During the freezing-thawing period, the $RMSE$ and AIC of the CAR-RR(FT) model were reduced by 0.0820 m and 46.0 in comparison with those of the CAR-RR model and the R^2 increased by 0.1453 in the validation period. When considering the results for the entire simulation period, the R^2 , $RMSE$, and AIC values were 0.8710, 0.1516 m, and -72.7 for the CAR-RR(FT) model, and 0.8230, 0.1896 m, and -23.8 for the CAR-RR model. These results demonstrated the better performance of the CAR-RR(FT) model, indicating that using the temperature during the freezing-thawing period improved the accuracy of the CAR-RR model. This is physically reasonable. Therefore, we used the temperature data during the freezing-thawing period later to predict the water table depth in the Hetao Irrigation District under water-saving scenarios.

Comparison of CAR-RR and CAR-SVR

When developing the machine-learning models, we observed that it is difficult for the CAR-RR and CAR-RR(FT) models to capture the peaks and troughs, especially in the validation period, as shown in Figure 4. We found that the SVR model outperforms the CAR models in terms of capturing the peaks and troughs. Generally speaking, for the hysteresis characteristics exhibited in the time series and the nonlinearity between the water table depth and independent variables, the CAR model considers the hysteresis characteristics, and the SVR model addresses the nonlinearity. This is shown in Figure 4, in which CAR-RR outperforms SVR because the hysteresis characteristics had a greater

Accepted Article

impact on the simulation, while considering the nonlinearity improved the SVR simulation accuracy for peaks and troughs. Based on these results, we developed the CAR-SVR model for simulating water table depth. The CAR-SVR model also uses the five independent variables used by CAR-RR with temperature as an additional variable during the freezing-thawing period. This model is denoted as CAR-SVR(FT). The results of using CAR-RR(FT) and CAR-SVR(FT) for simulating water table depth are shown in Figure 5. For the results of the entire simulation period, the R^2 , $RMSE$, and AIC values were 0.9553, 0.0706 m and -147.6, respectively, for the CAR-SVR(FT) model, and 0.8710, 0.1516 m, and -72.7, respectively, for the CAR-RR(FT) model. In summary, the CAR-SVR(FT) model obtained better results at the peaks and troughs than the CAR-RR(FT) models. The CAR-RR(FT) model obtained smaller peaks and troughs than the true values due to its intrinsic linearity while it can be used for prediction as a trade-off for model complexity and accuracy, since it can show the clear relationship between the dependent and independent variables.

Another concern is that the model ignored important variables as unrelated factors when learning data, as noted in the section titled Results of the CAR-RR model. Additionally, it is not true that the more the data, the better the model performance. The data should be pre-processed by considering physical background, which can ensure that predictions are more closely approximated to true value.

Variation of the water table depth under the water-saving policy

The improved model CAR-SVR(FT) can provide more accurate results of peaks and troughs when both strong nonlinearity of variables and hysteresis characteristics in time series exist, which was then used in prediction in this study. The predicted monthly water table depth by the CAR-SVR(FT) model under different levels of precipitation assurance with the same water diversion

and different water diversion conditions with a 50% level of precipitation assurance are shown in Figures 6(a) and 6(b). The precipitation showed very slight impacts on the water table depth prediction results as shown in Figure 6(a), whereas water diversion showed much stronger impacts.

The annual average water table depth and the maximum and minimum monthly water table depth for the crop growth period for the nine scenarios are illustrated in Figures 6(c)-6(e). The results showed that S9 resulted in a maximum average water table depth of 2.167 m. The water table depth was shallowest under S1 with a depth of 1.894 m, which was 0.078 m deeper than the current level. The descending order of the water table depth for the nine scenarios was as follows: $S9 > S8 > S7 > S6 > S5 > S4 > S3 > S2 > S1$, which demonstrated that the water diversion was the most important factor to influence the water table depth in this area. Under a 50% level of precipitation assurance, the average water table depth under current water diversion was 1.816 m, which was 2.060 m with the 4 billion m^3 water diversion and increased to 2.143 m with the 3.64 billion m^3 water diversion. The water table depth in the crop growth period (from May to September) under current water diversion was 1.433-2.103 m. It was 1.690-2.394 m with 4 billion m^3 water diversion, and 1.769-2.482 m with 3.64 billion m^3 water diversion. Through the test-pit experiment, the suitable water table depth of natural vegetation and crop was 1.5-1.8 m (Wang et al., 1993). When the water diversion was 3.64 billion m^3 , the water table depth was much deeper than the suitable depth, which may cause environmental problems and crop production reduction. The discrepancy of the minimum water table depth obtained from the CAR-SVR model and CAR-RR model ranged from -0.001m to 0.011m, and the discrepancy of average water table depth ranged from 0.06 m to 0.129 m, and the discrepancy of maximum water table depth ranged from 0.188 m to 0.311 m.

Conclusion

In this paper, we developed two new machine-learning models (CAR-RR and CAR-SVR) to simulate and predict the water table depth in arid agricultural areas that experience seasonal freezing and thawing with a planned water saving policy. Our work leads to the following major conclusions:

(1) The CAR-RR model outperforms the other machine-learning models, including, SVR and MLR, because CAR-RR considered the hysteresis characteristics in time series.

(2) The CAR-RR(FT) model had a better performance both during the freezing-thawing period and throughout the entire simulation period, when it considered temperature as an input data during the freezing-thawing period.

(3) The CAR-RR model failed to capture the peaks and troughs because of the model's intrinsic linearity. This problem can be resolved by integrating CAR with SVR model, which considers the nonlinearity between water table depth and input variables.

(4) The CAR-SVR(FT) model was used for water table depth prediction under future changing conditions. The prediction results showed that environmental problems and crop production reduction may be resulted when water diversion is 3.64 billion m³.

(5) When using the machine-learning methods, the data should be preprocessed by considering physical background.

(6) The CAR-RR can show clear relationship between the dependent and independent variables.

The model can be used for prediction as a trade-off for model complexity and accuracy.

Acknowledgments

The study was partially supported by Natural Science Foundation of China through Grants

51779178, 51790533, and 51629901, and the project of water conservancy science and technology plan in Inner Mongolia Autonomous Region (Grant No. 213-03-99-303002-NSK2017-M1). We thank Editor-in-Chief Henk M. Haitjema, the executive editor Yu-Feng Lin, and three anonymous reviewers for their constructive comments that helped improve the paper.

References

- Behzad, M., Asghari, K. and Coppola, E.A. 2010. Comparative Study of SVMs and ANNs in Aquifer Water Level Prediction. *Journal of Computing in Civil Engineering* 24, no. 5: 408-413.
- Behzad, M., Asghari, K., Eazi, M. and Palhang, M. 2009. Generalization performance of support vector machines and neural networks in runoff modeling. *Expert Systems with Applications* 36, no. 4: 7624-7629.
- Box, G. E. P., and G. Jenkins. 1976. Time Series Analysis: Forecasting and Control, 2nd ed. *Holden-Day*, San Francisco.
- Brunner, P., Cook, P.G. and Simmons, C.T. 2012. Hydrogeologic controls on disconnection between surface water and groundwater. *Water Resources Research* 45, no. 1: W01422.
- Chang, J., Li, S., Li, Z. and Xing, Y. 2008. Application of CAR and SVM to Prediction of Climatic Trend of Fog in Winter Half Year. *Meteorological and Environmental Sciences* 31, no. 1: 16-19 (in Chinese).
- Chen, Z., Grasby, S.E. and Osadetz, K.G. 2002. Predicting average annual groundwater levels from climatic variables: an empirical model. *Journal of Hydrology* 260, no. 1: 102-117.
- Coppola, E., Rana, A.J., Poulton, M.M., Szidarovszky, F., Uhl., V.V. 2005. A neural network model for predicting aquifer water level elevations. *Groundwater* 43, no. 2: 231-241.

Coppola, E., Szidarovszky, F., Poulton, M. and Charles, E. 2003. Artificial Neural Network Approach for Predicting Transient Water Levels in a Multilayered Groundwater System Under Variable State, Pumping, and Climate Conditions. *Journal of Hydrologic Engineering* 8, no. 6: 348-360.

Coulibaly, P., Anctil, F., Aravena, R. and Bobée, B. 2001. Artificial neural network modeling of water table depth fluctuations. *Water Resources Research* 37, no. 4: 885-896.

Daliakopoulos, I.N., Coulibaly, P. and Tsanis, I.K. 2005. Groundwater level forecasting using artificial neural networks. *Journal of Hydrology* 309, no. 1: 229-240.

Demirhan, H. 2014. The problem of multicollinearity in horizontal solar radiation estimation models and a new model for Turkey. *Energy Conversion and Management* 84: 334-345.

Ebrahimi, H. and Rajaei, T. 2017. Simulation of groundwater level variations using wavelet combined with neural network, linear regression and support vector machine. *Global and Planetary Change* 148: 181-191.

Feng, S., Huo, Z., Kang, S., Tang, Z. and Wang, F. 2011. Groundwater simulation using a numerical model under different water resources management scenarios in an arid region of China. *Environmental Earth Sciences* 62, no. 5: 961-971.

Huang, S., Chang, J., Huang, Q. and Chen, Y. 2014. Monthly streamflow prediction using modified EMD-based support vector machine. *Journal of Hydrology* 511, no. 7: 764-775.

Jha, M.K. and Sahoo, S. 2015. Efficacy of neural network and genetic algorithm techniques in simulating spatio-temporal fluctuations of groundwater. *Hydrological Processes* 29, no. 5: 671-691.

Khan, M.S. and Coulibaly, P. 2006. Application of Support Vector Machine in Lake Water Level Prediction. *Journal of Hydrologic Engineering* 20, no. 11: 199-205.

Knapp, K.C., Weinberg, M., Howitt, R. and Posnikoff, J.F. 2003. Water transfers, agriculture, and groundwater management: a dynamic economic analysis. *Journal of Environmental Management* 67, no. 4: 291-301.

Kuo, J.T., Hsieh, M.H., Lung, W.S. and She, N. 2007. Using artificial neural network for reservoir eutrophication prediction. *Ecological Modelling* 200, no. 1: 171-177.

Li, R., Shi, H, Flerchinger G N, Takeo Akae, Wang, C. 2012. Simulation of freezing and thawing soils in Inner Mongolia Hetao Irrigation District, China. *Geoderma* 173-174: 28-33.

Lilliefors, H.W. 1967. On the Kolmogorov-Smirnov Test for Normality with Mean and Variance Unknown. *Publications of the American Statistical Association* 62, no. 318: 399-402.

Maheswaran, R. and Khosa, R. 2013. Long term forecasting of groundwater levels with evidence of non-stationary and nonlinear characteristics. *Computers & Geosciences* 52, no. 1: 422-436.

Makridakis, S., Wheelwright, S. and Hyndman, R.J. 2008. Forecasting: Methods and Applications, 3rd Edition. Wiley, Singapore.

Manzione, R.L., Wendland, E. and Tanikawa, D.H. 2012. Stochastic simulation of time-series models combined with geostatistics to predict water-table scenarios in a Guarani Aquifer System outcrop area, Brazil. *Hydrogeology Journal* 20, no. 7: 1239-1249.

Mohanty, S., Jha, M.K., Kumar, A. and Panda, D.K. 2013. Comparative evaluation of numerical model and artificial neural network for simulating groundwater flow in Kathajodi–Surua Inter-basin of Odisha, India. *Journal of Hydrology* 495, no. 15: 38-51.

Moosavi, V., Vafakhah, M., Shirmohammadi, B. and Ranjbar, M. 2014. Optimization of Wavelet-ANFIS and Wavelet-ANN Hybrid Models by Taguchi Method for Groundwater Level Forecasting. *Journal for Science and Engineering* 39, no. 3: 1785-1796.

Nayak, P.C., Rao, Y.R.S. and Sudheer, K.P. 2006. Groundwater Level Forecasting in a Shallow Aquifer Using Artificial Neural Network Approach. *Water Resources Management* 20, no. 1: 77-90.

Nourani, V., Mogaddam, A.A. and Nadiri, A.O. 2008. An ANN-based model for spatiotemporal groundwater level forecasting. *Hydrological Processes* 22, no. 26: 5054-5066.

Raghavendra, N.S.; Deka, P.C. 2014. Support vector machine applications in the field of hydrology: A review. *Applied Soft Computing Journal* 19, no. 6: 372-386.

Ravansalar, M., Rajaei, T. and Kisi, O. 2017. Wavelet-linear genetic programming: A new approach for modeling monthly streamflow. *Journal of Hydrology* 549: 461–475.

Rezaie-Balf, M., Naganna, S.R., Ghaemi, A. and Deka, P.C. 2017. Wavelet coupled MARS and M5 model tree approaches for groundwater level forecasting. *Journal of Hydrology* 553: 356-373.

Rodell, M., Velicogna, I. and Famiglietti, J.S. 2009. Satellite-based estimates of groundwater depletion in India. *Nature* 460: 999-1002.

Russo, T.A. and Lall, U. 2017. Depletion and response of deep groundwater to climate-induced pumping variability. *Nature Geoscience* 10, no. 2: 105-108.

Sahoo, S. and Jha, M.K. 2013. Groundwater-level prediction using multiple linear regression and artificial neural network techniques: a comparative assessment. *Hydrogeology Journal* 21, no.8: 1865-1887.

Sahoo, S., Russo, T.A., Elliott, J. and Foster, I. 2017. Machine learning algorithms for modeling groundwater level changes in agricultural regions of the U.S. *Water Resources Research* 53, no. 5: 3878-3895.

Satchithanantham, S., Krahn, V., Ranjan, R.S. and Sager, S. 2014. Shallow groundwater uptake and irrigation water redistribution within the potato root zone. *Agricultural Water Management* 132, no. 3: 101-110.

Schoups, G. et al. 2005. Sustainability of irrigated agriculture in the San Joaquin Valley, California. *Proceedings of the National Academy of Sciences of the United States of America* 102, no. 43: 15352-15356.

Shah, T., Bovolo, C.I., Parkin, G. and Sophocleous, M. 2009. Climate change and groundwater: India's opportunities for mitigation and adaptation. *Environmental Research Letters* 4, no. 3: 375-383.

Shiri, J., Kisi, O., Yoon, H., Lee, K.K. and Nazemi, A.H. 2013. Predicting groundwater level fluctuations with meteorological effect implications — A comparative study among soft computing techniques. *Computers & Geosciences* 56(C): 32-44.

Shirmohammadi, B., Vafakhah, M., Moosavi, V. and Moghaddamnia, A. 2013. Application of Several Data-Driven Techniques for Predicting Groundwater Level. *Water Resources Management* 27, no. 2: 419-432.

Suryanarayana, C., Sudheer, C., Mahammood, V. and Panigrahi, B.K. 2014. An integrated wavelet-support vector machine for groundwater level prediction in Visakhapatnam, India. *Neurocomputing* 145, no. 18: 324-335.

Tang, Q. 2010. Data Processing System--Experimental Design, Statistical, Analysis and Data Mining. *Science Press*, Beijing (in Chinese).

Vapnik, V. 1995. The nature of statistical learning theory. *Springer*.

Wang, L. et al. 2016. Spatial and Temporal Variations of Streambed Vertical Hydraulic Conductivity in the Weihe River, China. *Water* 70, no. 8.

Wang, L., Chen, Y. and Zeng, G. 1993. Irrigation Drainage and Salinization Control in Neimenggu Hetao Irrigation Area. *Water Resources and Electric Power Press*, Beijing. (in Chinese).

Wei, O., Liu, B., Wu, Y. 2016. Satellite-based estimation of watershed groundwater storage dynamics in a freeze-thaw area under intensive agricultural development. *Journal of Hydrology* 537: 96-105.

Yang, W. et al. 2017. Groundwater dynamics forecast under conjunctive use of groundwater and surface water in seasonal freezing and thawing area. *Transactions of the Chinese Society of Agricultural Engineering* 33, no. 4: 137-145 (in Chinese).

Yang, Z.P., Lu, W.X., Long, Y.Q. and Li, P. 2009. Application and comparison of two prediction models for groundwater levels: A case study in Western Jilin Province, China. *J. Journal of Arid Environments* 73, no. 4-5: 487-492.

Yao, J., Liu, Z., Yang, Q., Meng, X. and Li, C. 2014. Responses of runoff to climate change and human activities in the Ebinur Lake Catchment, western China. *Water Resources* 41, no. 6: 738-747.

Yoon, H., Hyun, Y., Ha, K., Lee, K.K. and Kim, G.B. 2016. A method to improve the stability and accuracy of ANN- and SVM-based time series models for long-term groundwater level

predictions. *Computers & Geosciences* 90(PA): 144-155.

Yoon, H., Jun, S.C., Hyun, Y., Bae, G.O. and Lee, K.K. 2011. A comparative study of artificial neural networks and support vector machines for predicting groundwater levels in a coastal aquifer. *Journal of Hydrology* 396, no. 1: 128-138.

Zhang, X., Peng, Y., Zhang, C. and Wang, B. 2015. Are hybrid models integrated with data preprocessing techniques suitable for monthly streamflow forecasting? Some experiment evidences. *Journal of Hydrology* 530: 137-152.

Zhang, Z., Liang, Z., Feng, B., Huang, J. and Dong, W.U. 2017. Groundwater level forecast based on principal component analysis and multivariate time series model. *Advances in Water Science* 28, no. 03: 415-420 (in Chinese).

Zhu, Y., Shi, L., Lin, L., Yang, J. and Ye, M. 2014. A fully coupled numerical modeling for regional unsaturated-saturated water flow. *Journal of Hydrology* 475, no. 26: 188-203.

Figure Captions

Figure 1. Study area and the groundwater observation wells.

Figure 2. Time serious of monthly measurements and standardized variables of (a) water diversion, (b) precipitation, (c) evaporation, (d) water drainage, (e) temperature, and (f) water table depth.

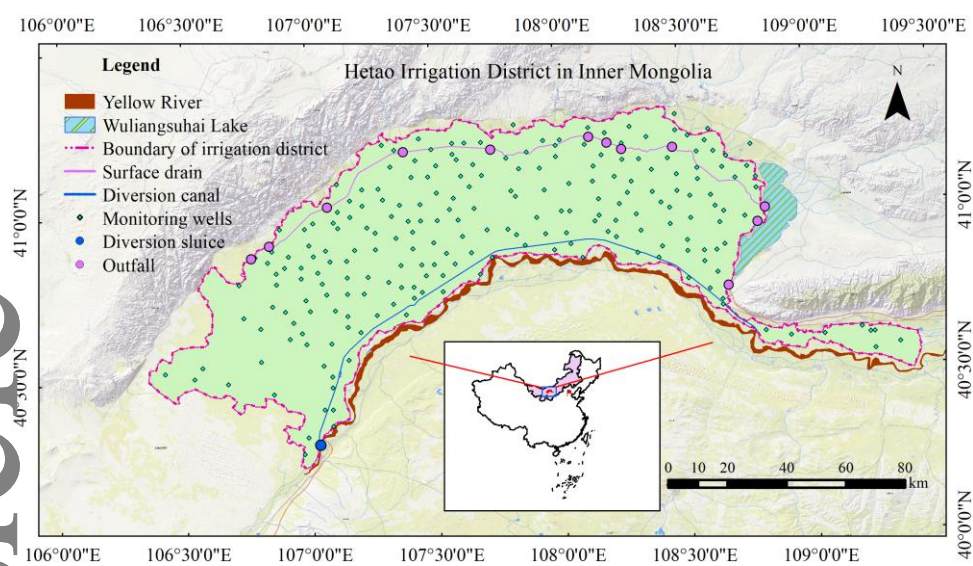
Figure 3. The flow chart of the CAR-RR and CAR-SVR models.

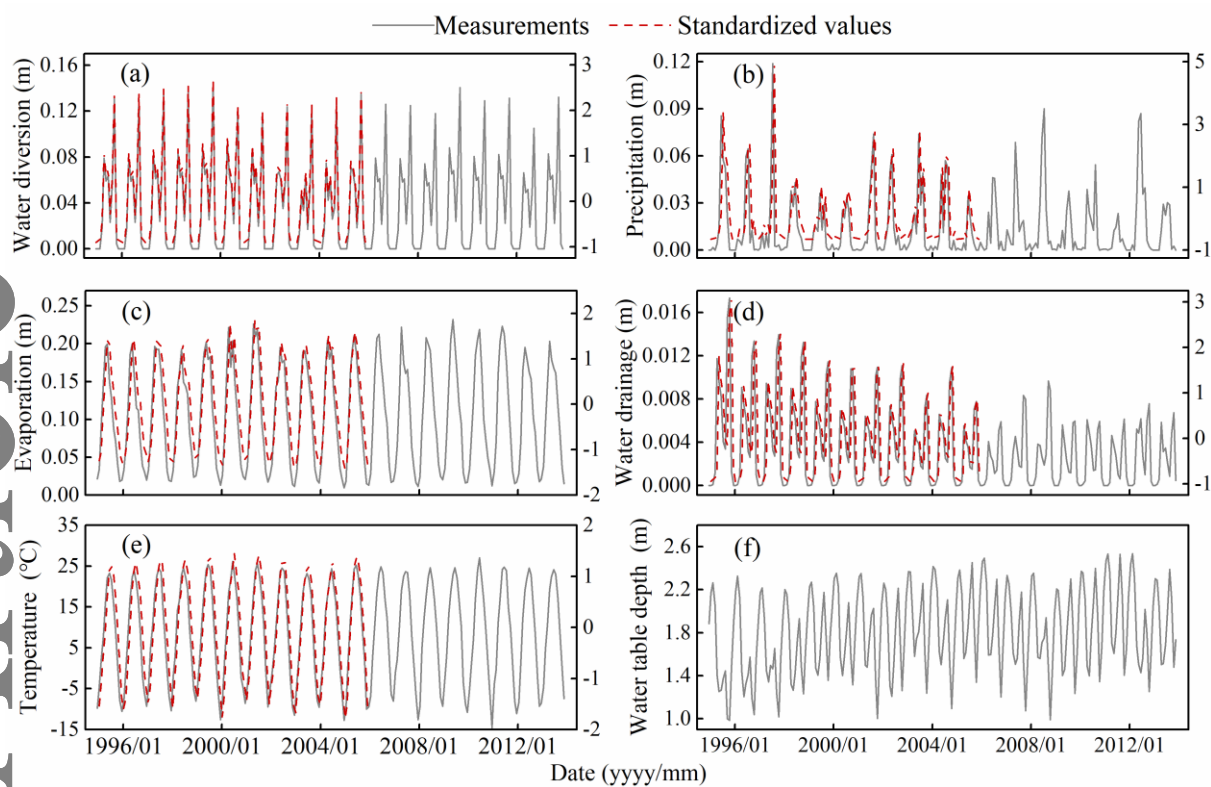
Figure 4. The comparison results of simulated and measured water table depth in the calibration and validation periods.

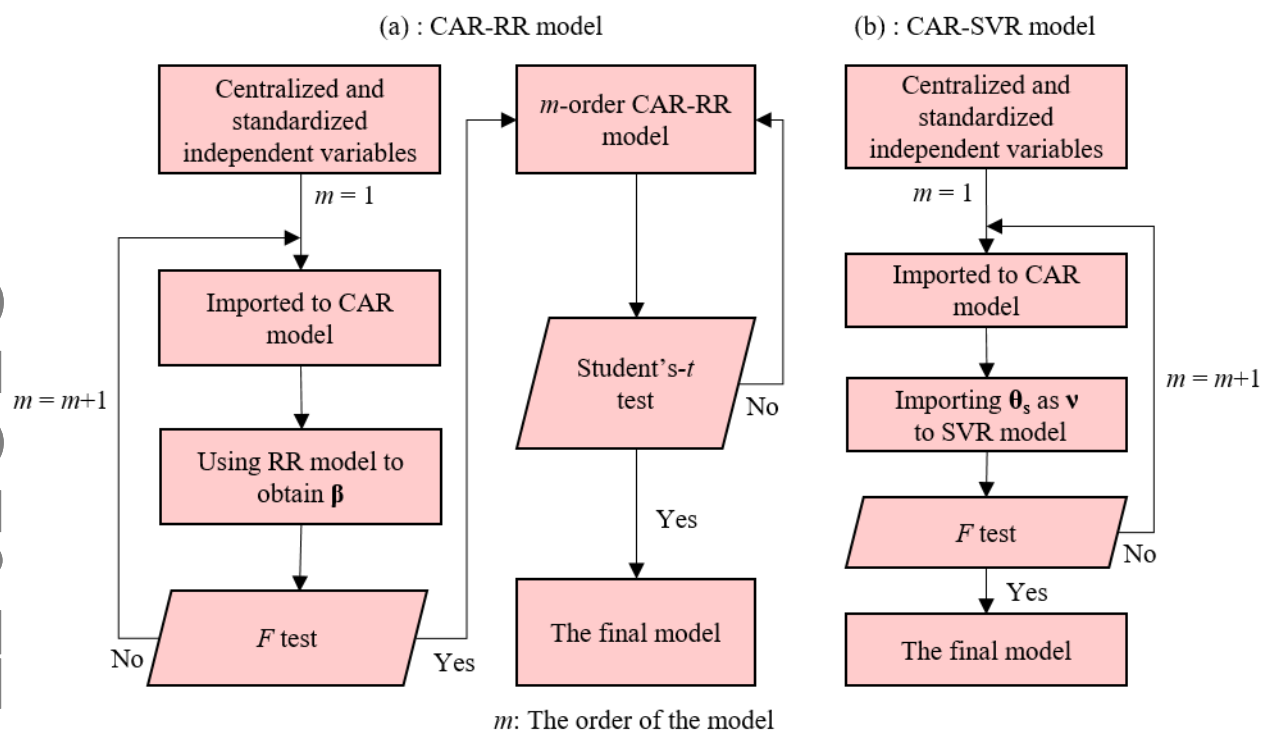
Figure 5. The comparison results of calculated and simulated water table depths by the CAR-RR(FT) and the CAR-SVR(FT) models.

Figure 6. The monthly water table depth under different (a) levels of precipitation assurance with the same water diversion and (b) water diversion conditions with a 50% level of precipitation assurance; (c) the mean, (d) maximum, and (e) minimum variation of water table depth under the nine scenarios.

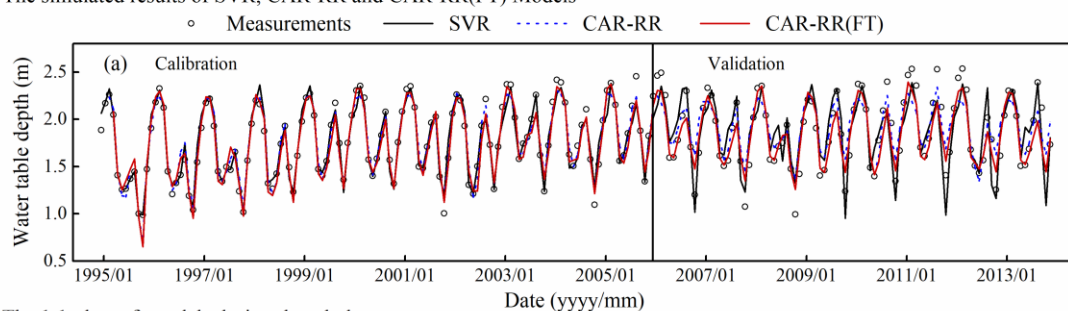
Notes: * represents the whole year; ** is the crop growth period.



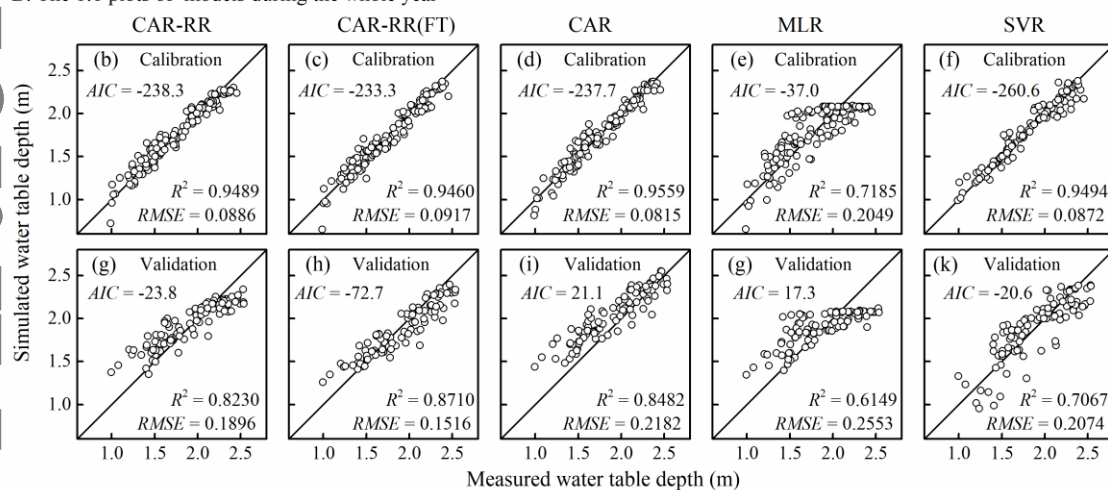




A: The simulated results of SVR, CAR-RR and CAR-RR(FT) Models



B: The 1:1 plots of models during the whole year



C: The 1:1 plots of models during the freezing-thawing period

